Integrating Pulsed High Power Light Emitting Diodes for Schlieren Imaging

By

Hanah Choice
Department of Mechanical Engineering
Cockrell School of Engineering

Undergraduate Engineering Honors Thesis
The University of Texas
Spring 2018

Noel T. Clemens, Ph.D.
Department of Aerospace Engineering and Engineering Mechanics

---

Leon Vanstone, Ph.D.
Department of Aerospace Engineering and Engineering Mechanics
Second

Acknowledgements

First, I would like to thank Dr. Noel Clemens for being so welcoming when I first expressed interest in this field of research. I would also like to thank him for allowing me to do an honors thesis and being my first reader. I would also like to thank Leon Vanstone for giving me this project at the Pickle Research Campus Lab, as well as agreeing to be my second reader. I built this LED box with Pablo Cortez with his expertise in electronics. Although we were both new to this circuit design, Pablo was unfazed throughout all stages of this project and was so generous with sharing his time and knowledge. He taught me so much about circuit building and soldering. I'd also like to thank Serdar Seckin for allowing me to use his schlieren and shadowgraph images from the undergraduate lab he teaches. I am also grateful to Geetha Rajagopal for being so responsive with ordering parts with each iteration of the project, she was especially patient about ordering additional spare parts when components would break. Finally, I would like to thank the people who run the machine shops of both Mechanical Engineering and Aerospace Engineering departments. They were extremely helpful with pointing out the tools I needed to make the required modifications possible. Without all these people, the completion of this honors thesis would not have been possible.

Integrating Pulsed High Power Light Emitting Diodes for Schlieren Imaging

Hanah A. Choice
The University of Texas at Austin, 2018

Supervisor: Noel T. Clemens, Ph.D.

Abstract

This honors thesis describes the development of a light source for schlieren imaging that is based on pulsed high-brightness light emitting diodes. Schlieren imaging is an optical technique that enables the visualization of density gradients in flows. The work involves the customization and fabrication of the circuit for the purpose of imaging of supersonic wind tunnel flows and includes the design of the circuit enclosure and the integration of the lamp into the schlieren system. The final product is demonstrated in the High-Speed Wind Tunnel at the J.J. Pickle Research Campus at UT Austin. Several prototypes were tried, and the final design offers a safe, easy to use pulsed light source, which can be integrated into many schlieren systems.

Table of Contents

Nomenclature

κ Von Kármán constant

M Mach number

p pressure

Pr Prandtl number

r recovery factor

Re Freestream Reynolds number, length scale is streamwise distance from plate leading edge

T temperature

u streamwise velocity

p friction velocity

x streamwise coordinate

y coordinate normal to plate

γ ratio of specific heats

δ boundary layer thickness based on 99% velocity profile

δ^* displacement thickness

η y⁄δ

μ dynamic viscosity

Π coefficient of wake function

ρ density

τ shear stress

ν kinematic viscosity

λWavelength

n Index of refraction

f Focal length

A current

V voltage

Ω resistance

P power

Chapter 1

Introduction

1.1 Motivation

The motivation for this project came from the need to develop a high power, high repetition rate (kHz) pulsed light source to enable the visualization of high-speed flow dynamics using the schlieren imaging technique. Light emitting diodes (LEDs) are an excellent solution to this problem since they can provide a lag free light source that can be pulsed at high repetition rates. Schlieren imaging is a type of flow diagnostic that enables the visualization of density gradients. At the Pickle Research Campus High Speed Wind Tunnel Laboratory, one of the research areas include wind tunnel experiments to observe shockwave boundary layer interactions for applications related to supersonic and hypersonic flight. While quantitative data, such as temperature and pressure, is crucial, having a reliable means to visualize the locations of such structures as shocks, expansion waves, boundary layers and shear layers, is critical to get a comprehensive understanding of what is occurring in the flow. The goal of this project is to develop a light source that enables the visualization of the time-dependent nature of these flows at framing rates that are fast enough to resolve the unsteady dynamics.

1.2 Project Objectives

This project has two main objectives that I hoped to solve through my research. The first was to design, build and test a refined prototype that was stable and easy enough for any researcher to use safely and with minimal assistance. The second was to perform various endurance tests on my design to gauge and validate high-duty cycle use of the circuit and its components. Since wind tunnel tests are often a minute in length, I wanted to ensure that repeated use with minimal cooling-off time was possible for the design. This required a larger safety margin on various components including the LEDs and low resistance resistors used for heat dissipation.

Chapter 2

Background

2.1 Shock waves

A shock wave is a type of propagating disturbance. If the motion of an object through air is subsonic (i.e. slower than the speed of sound), the air molecules before the object's surface will move out of the way away from the object to avoid it. The approaching gas molecules are able to adjust because pressure waves propagate upstream to "warn" them of the disturbance ahead. However, once the object reaches the speed of sound or exceeds it, the pressure waves cannot travel fast enough to "warn" the air molecules of the approaching disturbance and a shock wave forms. The air cannot adjust to its presence as it moves through the air therefore it abruptly adjusts, and this occurs through shock waves [1]. The shock wave is the accumulation of the pressure waves and presents itself as a very thin region in the flow where supersonic flow is decelerated to subsonic flow.

Figure 1 lists how the gas properties are affected across a shock. Velocity and Mach number abruptly decrease across a shock, whereas static pressure, temperature, and gas density increase. Figure 2 shows normal and oblique shock waves. A normal shockwave is perpendicular to the flow direction where supersonic flow enters the wave and subsonic flow exits [1]. Oblique shock waves are inclined at any angle and are usually observed at the leading edge of a sharp body. An application of oblique shocks can be found in aircraft design where they are utilized to achieve more favorable post-shock conditions in comparison to single normal shocks.

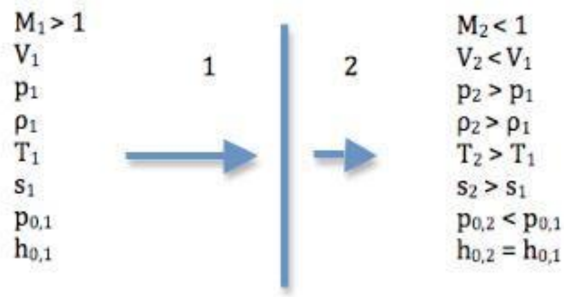

Figure 1. “Shock.” *Georgia Tech Fixed Wing Dsecondesign Class Wiki*, gtae6343.wikia.com/wiki/Shock.

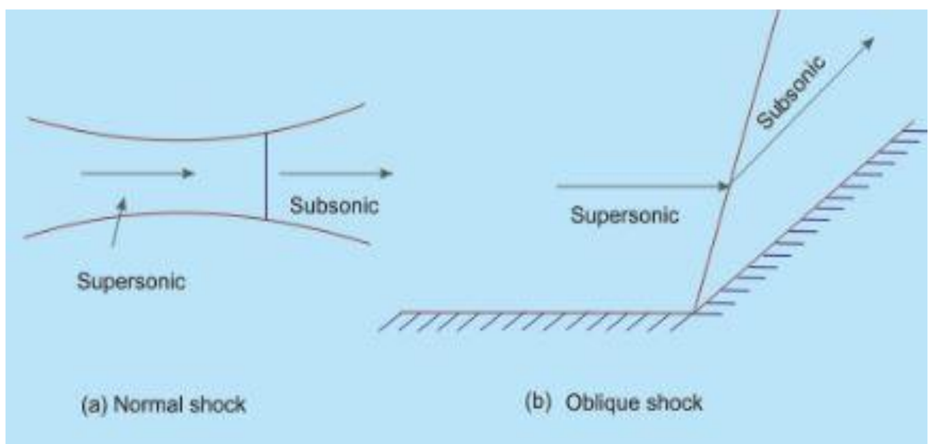

Figure 2. “Compressible Flow.” National Programme on Technology Enhanced Learning. 10 May 2018.

To understand what shockwave boundary layer interactions are, first boundary layers should be defined. A boundary layer is a thin region next to a surface where viscous forces are important and there exist large gradients in velocity. At the wall the velocity is zero, owing to the no-slip condition. The velocity profile through the boundary layer is therefore zero at the wall and gradually transitions to the free-stream velocity at the edge of the boundary layer. Boundary layers are associated with skin friction drag, convective heat transfer, and when they separate on wings are associated with aerodynamic stall [7]. An example of this profile can be seen in Figure 3.

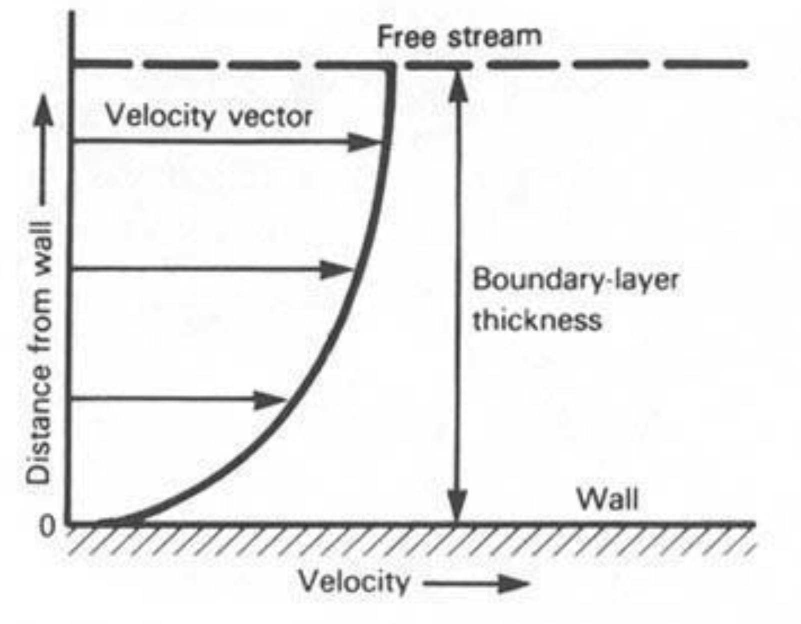

Figure 3. *Profile of a boundary layer. (NASA EP-89, 1971, p. 68)*

When shock waves and boundary layers interact, it introduces a whole new flow phenomenon (Delery, 1). The adverse pressure gradient associated with the shock wave can be strong enough to cause boundary layer separation, as can be seen in Figure 4 (Delery, 1). The resulting separated flow is highly unsteady. The unsteadiness that comes with this interaction is a major focus of research for shock wave boundary layer interactions (SWBLI). Since SWBLI occur in all transonic, supersonic, and hypersonic vehicles, the research gathered from understanding more about their impact and control is useful for potential applications in design considerations for hypersonic aircraft components [6].

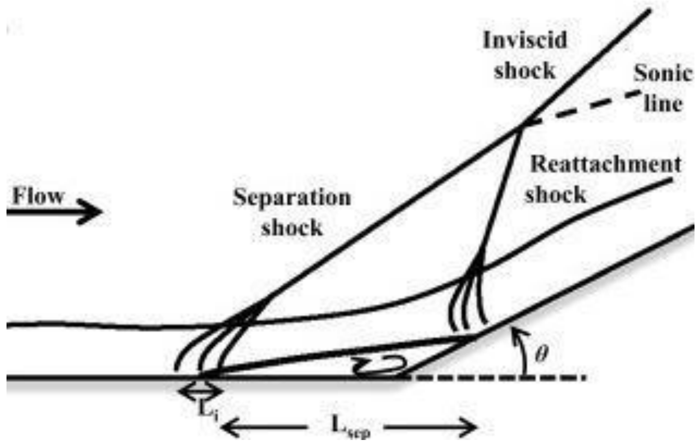

Figure 4. Gaitonde, Datta V. "Progress in Shock Wave/Boundary Layer Interactions." *43rd Fluid Dynamics Conference*, 22 Jan. 2013, doi:10.2514/6.2013-2607.

2.2 Schlieren Imaging

Shock waves can be effectively visualized by the schlieren technique owing to the large density gradients associated with them. In schlieren imaging, the ability to observe the density gradient is dependent on changes to the index of refraction of the medium that the electromagnetic waves are propagating through (Schlieren, 1). The index of refraction, n, is the ratio of the speed of light in a vacuum to the speed of light in a specified medium. In the case for schlieren imaging, changes to the value of n are caused by the refraction of waves through a medium that is the test section of high speed air flow.

Figure 5 shows the path of the light rays in a schlieren set up. The light rays emanating from a point light source are directed to a concave mirror and thus become collimated (parallel). Assuming that the light rays are of the same wavelength, they reflect at the same angle. The medium being studied is the air flow in the test section where the light rays are refracted. The other mirror, located after the test section, collects the remaining parallel rays and focuses them to a point at the knife edge located before the camera. The light rays that were refracted through the medium are represented as dashed lines. As seen in Figure 5, the dashed lines miss the focal spot and are blocked by the knife edge, a type of spatial filter. The camera detects the missing rays as darkened lines. The darkened lines denote where the density gradients occur, which is how shock waves are detected [6].

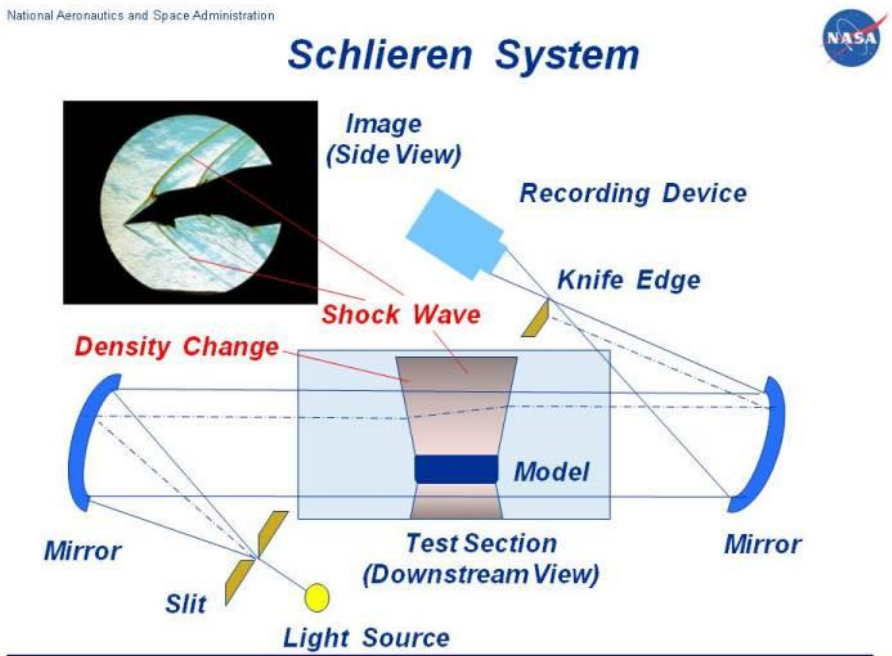

Figure 5. "Schlieren System." NASA, 15 May 2015,www.grc.nasa.gov/www/k-12/airplane/tunvschlrn.html.

The knife edge is crucial to providing the contrast in light intensity. The knife edge blocks a portion of the focal spot and thus renders the image at half intensity. If light rays are deflected towards the knife edge, the part of the image where those light rays originate from will be darkened. This will stand out in parts of the image with constant density, hence the contrast. In addition, if the light rays are deflected away from the knife edge, that part of the image will appear brighter than unaffected regions of the image (Schlieren, 1). This variation in intensity based on the direction and magnitude of the density gradients is how schlieren systems enable visualization of shock waves.

To increase the sensitivity of the schlieren setup, there are two ways to do this. The first is to make the focal length of the mirror placed after the cross section medium longer. The second is to decrease the size of the point source of light increases the sensitivity as well.

2.2.1 Light Sources

The reason the size of the point source matters is that the larger the source, the less collimated the resulting light beam is. This is shown schematically in Figure 6.

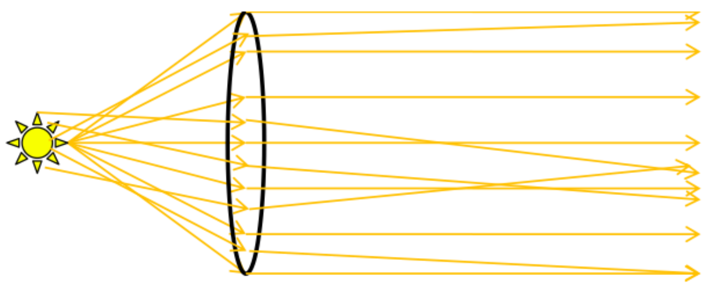

Figure 6. “Schlieren.” ASE 162 M.

The consequence of non-collimated rays is blurred images, because the non-collimated rays do not focus to a small focal spot. Some light sources emit white light, which can lead to different colors being refracted differently, as seen in Figure 7, and thus can lead to blurring. Since white light contains all wavelengths, it may be necessary to use a filter to create a more monochromatic light source.

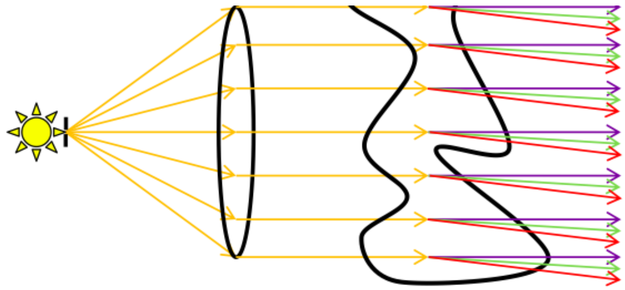

Figure 7"Schlieren." ASE 162 M.

Traditionally, the light sources used are flash lamps or pulsed lasers. The disadvantage with flash lamps is their light emissions come with a delay. This can be seen in Figure 8 where the time trace of light emission for a high-power LED (left) and a conventional xenon flash lamp (right) in response to a trigger pulse (bottom) is shown [9]. The decay of the flash lamp displays exponential behavior while the decay of the LED is distinct and in sync with the drive pulse. The non-constant light emissions results in smeared images, and given that the camera operates at a high frame rate, this leads to the collection of many smeared images with each experimental run. Another advantage the LED has over the flash lamp is that the duration of its light emission can be modified by the pulse width of the input drive pulse [9]. In contrast, the pulse width of the flash lamp cannot be adjusted.

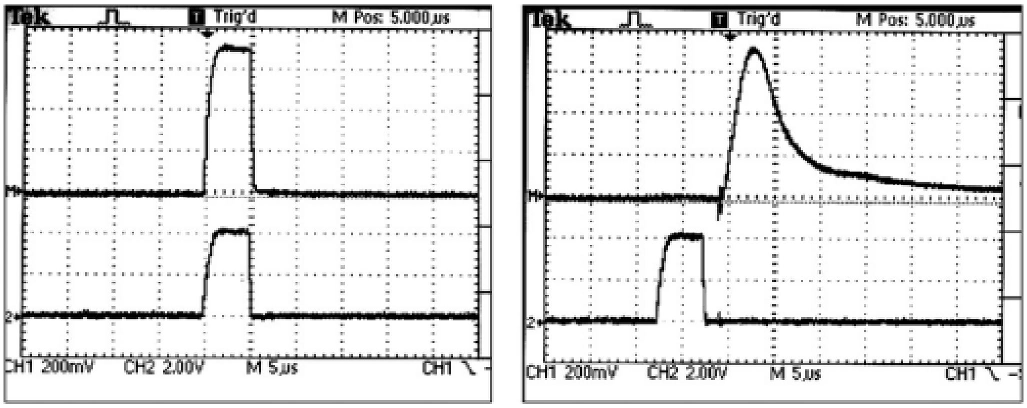

Figure 8: Willert, C, et al. “Pulsed Operation of High-Power Light Emitting Diodes for Imaging Flow Velocimetry.” Measurement Science and Technology, vol. 21, no. 7, Aug. 2010, p. 075402., doi:10.1088/0957-0233/21/7/075402.

LEDs provide “a significantly more stable pulse to pulse light output in both intensity and spatial intensity distribution” in comparison to traditional laser illumination [3]. LEDs are being explored for the ability to match the pulse-to-pulse intensity with the frame rate of the camera. The narrow emission bandwidth of LEDs reduces chromatic aberrations, yet it is spectrally wide enough to prevent the appearance of speckle and diffraction effects in the images [9]. Researchers today are using high power pulsed LEDs with varying pulsed LED driver configurations. The circuit of which this project based on was sourced by a paper published by C. Willert. To avoid the cost of a high expense fast laser diode driver to generate the pulses to drive the LED, the circuit shown in Figure 5 provides a relatively inexpensive system to drive the pulse.

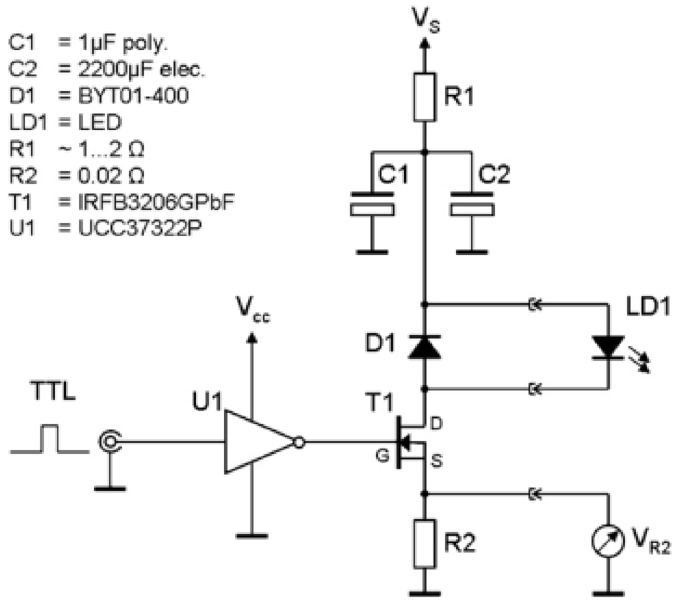

Figure 9. Willert, C, et al. "Pulsed Operation of High-Power Light Emitting Diodes for Imaging Flow Velocimetry." Measurement Science and Technology, vol. 21, no. 7, Aug. 2010, p. 075402., doi:10.1088/0957-0233/21/7/075402.

The circuit is made up of the following components: two voltage sources, two capacitors, two resistors, a MOSFET power transistor, a diode, and an LED. A power supply of 24 V was used for the main voltage supply, V_s, to charge the capacitors. Capacitors are devices used to store an electric charge, consisting of one or more pairs of conductors separated by insulators. Resistors are devices with a designed resistance to the passage of an electric current. The purpose of R_1 (resistor following V_s) is to limit the charging current of the capacitor bank in between the current pulses and act as a rudimentary method of overcurrent protection in case the LED is accidentally operated in continuous mode [9]. The purpose of R_2 is for diagnostic purposes; measuring the voltage of R_2 gives the current of which the circuit is running at with Ohm's Law. Equation 3 shows that voltage is equal to current multiplied by the resistance. This is useful to the user in the case he or she wants to know the current at which the circuit is running at. All that is required are connections to the ends of R_2 with a multimeter or oscilloscope. D_1, the diode in parallel with the LED, is there to prevent the reversal of current to the LED during the rapid switching of the circuit.

$$V = I * R \qquad \text{Equation 7}$$

The voltage source first charges the capacitors which, once fully charged, powers the MOSFET transistor and triggers the gate to the MOSFET driver circuit. A square TTL signal is input to the driver circuit while the LED is connected to the drain of the power transistor. This configuration circuit acts as a switched constant-current source for the LED to be pulsed at.

2.2.2 CBT-120 LED Light Source

The light source used in the paper was Luminus's CBT 120 green LED. The light source was selected for the following reasons: high optical output, high thermal conductivity package, and uniform emission. Green was chosen because it outputs over 2000 lumens of light. A lumen is the SI unit of luminous flux. Green provides 30% more light than red LEDs and was found to provide brighter images because of a higher sensitivity of the camera detector.

Chapter 3

Experimental Set-Up and Testing

3.1 Early Prototypes

The LED circuit from the Willert paper was followed with several modifications. The paper's objective was to drive the LED at 120 amps, the max current. The LED (CBT 120) is rated for 27 Amps continuously, but the author wanted to determine at what duty cycle and frequency the LED could run without damaging the LED. The limiting factor of the current value that the LED runs at is the main voltage source. There are two voltage sources, one of which is for the gate driver which is responsible for sending the TTL signal to the gate of the MOSFET. A 24 V supply was selected as the main voltage source due to what was available in the electronics room at the PRC. The first prototype was to ensure that the circuit would work and if the power supply was sufficient for its intended purpose, it would be unnecessary to source out a more expensive one. The first prototype reiterated the circuit diagram in the Willert paper with changes to the resistance values. R_1 and R_2 in the paper were respectively 1 Ω and 0.2 Ω. However different resistor values were used from the paper as 120 A is not required for the light source. In order for the circuit to run at 120 A, the frequency at which the circuit could be operated would be significantly slower. And given that the purpose of this LED replacement is so that it can be run at the same frequency at which the camera is run at, the starting resistance values were conservatively 10 $\Omega$and 5 Ω, respectively for R_1 and R_2. With these resistance values, the current running was 1.6 A. Given that this was still the experimental phase of putting the circuit together, caution was taken to prevent the LED, the most expensive component of the circuit, from burning out. The goal of this project was to build this circuit and make the required modifications so that the circuit can run at the adequate current to obtain high quality schlieren images by determining its current pulse damage threshold. Therefore, choosing the resistance values was an iterative process.

The first prototype also used a National Instruments Elvis board, but this introduced problems when it came to test the circuit. At times when the LED would not turn on, it was difficult to diagnose if the circuit was not wired correctly, there were faulty components, or there was a lack of wiring contact. Troubleshooting was time intensive and it took the melting of a gate driver to move onto building the second prototype.

The second prototype was constructed once it was known that the circuit was in fact working. This time a circuit board was used, and direct contact was ensured due to the soldered connections. To provide more intensity, the resistance values were further decreased to 3.9 Ohms and 2.3 Ohms respectively for R_1 and R_2. A mistake made in the first prototype was not using resistors rated for high wattage as components heated up quickly. These new resistors were rated for 25 Watts each.

With this prototype, there was a considerable increase in light intensity, with 4.6 A. However, concerns with heat dissipation became a concern before increasing the LEDs intensity any further.

Figure 10 shows the second prototype with unideal cable management. When assembling the circuit, the LED, the circuit board, and the voltage supply had to be carefully moved because the wires were permanently connected. In addition, both prototypes did not have any method of heat dissipation other than the resistors.

Figure 10.

Researchers at the PRC brought up also brought up safety issues. If the LED were to be accidentally run continuously without the gate driver working, the LED would burn out. It was requested that anybody could use it with ease, and so to prevent any electrical shock, it was also requested that no exposed wires would be present. With these concerns, the following section follows.

3.2 Improved Features

After the testing of first and second prototype combined with the feedback given from researchers at the PRC, the following areas were modified: safety precautions, heat dissipation, and circuit packaging. Once it was recognized that this circuit was ready to be packaged into a box, the circuit was remade on to a copper circuit board.

Pin 3 of the gate driver is for the enable mode. Modifications were made to the circuit to where the MOSFET power transistor would not switch on if the TTL signal was not running. In addition, a switch was added to power the circuit on and off rather than rely on plugging in the voltage supply. Clear labels were also added to make it easy for the user.

For heat dissipation, a heat sink was added to the MOSFET power transistor as seen in Figure H. R1 and R2 are thermal pasted and screwed to the box the circuit is contained in for heat dissipation as well. The circuit was purposely packaged so that the fan will create cross flow across the circuit board and the resistors. Mesh panels were added at the end of the box for warm air to pass through. Warm air circulating in a sealed box would be cause poor cooling of the components and overheating. A unique feature added to this LED box was including a high and low mode. The final resistor values for R1 alternate between 1 Ω and .5 Ω and R2 with .5 Ω. The reason for this was to test if 1Ω would be provide enough light intensity, and if not, the circuit could easily switch .5 Ω without having to swap and desolder resistors.

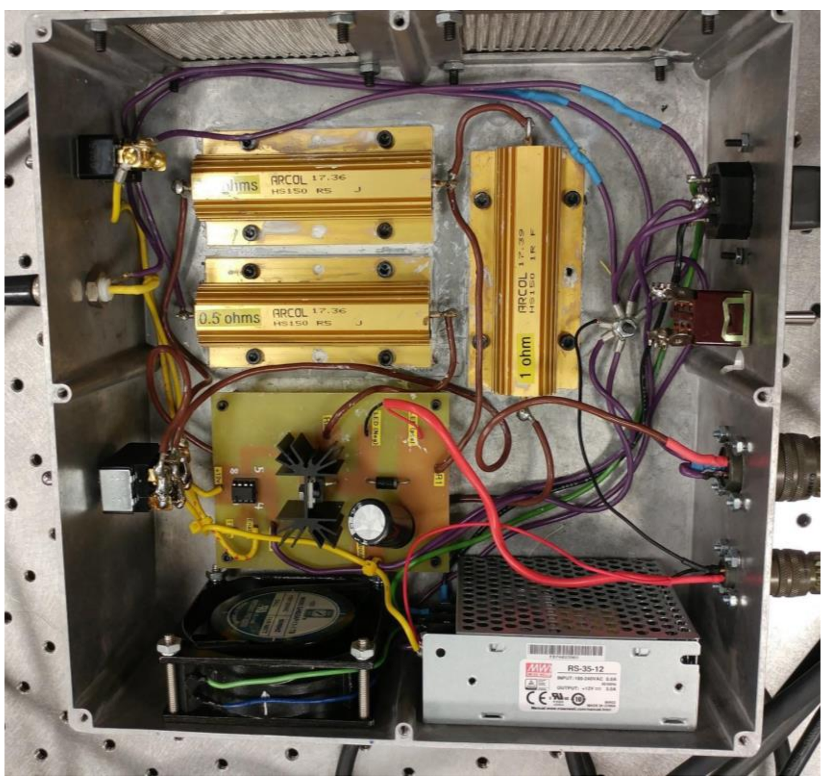

Figure 11. Final LED Box Configuration

Another feature that was added to make this box easy to use was putting all the cables and switches to one side of the box.

Finally, to make this package easily portable without having to carry the LED and voltage supply at the same time or require multiple people, cable pin connectors were added so that the cable for the voltage supply and LED could be removed and reattached easily. The use of pin connectors was to ensure solid contact between the wires.

3.3 Manufacturing

We utilized an all-aluminum project enclosure to house the many components for the LED circuit. Aluminum has many qualities that make it ideal for this situation. Its high thermal conductivity allows the enclosure to be effectively used as a large heat sink without having to purchase separate heat sinks for the resistors. It also is easier to machine than steel or other composites while still being relatively cheap. Caution was taken to make sure there were no exposed wires, heat shrink was also added in between the soldered connections to the pin connectors. All wires were double checked to be non-exposed, the circuit board was raised as well so no metal contact was made with any portion of the circuit board. This was accomplished by drilling four holes at corners of the board and screwing standoffs into the box.

The LED itself was thermally pasted to an aluminum heat sink for heat dissipation purposes. The board of the LED had pre made holes for mounting purposes as seen in Figure 13. Two holes were machined on the mill so that the mounting to the heat sink could be perfectly aligned.

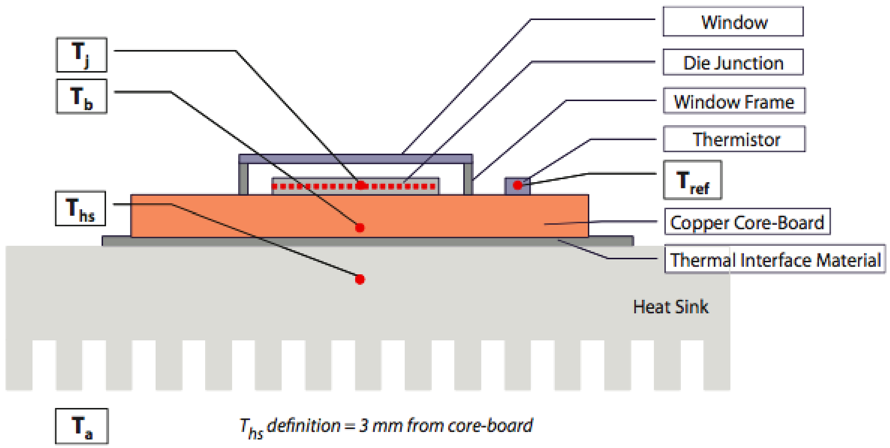

Figure 12. Luminus (2009) Product Data Sheet, PhlatLight PT120 Projection Chipset. Luminus Devices Inc

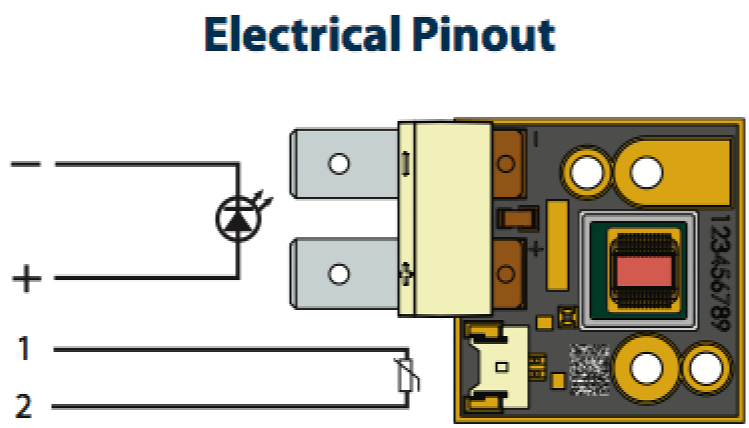

Figure 13. Luminus (2009) Product Data Sheet, PhlatLight PT120 Projection Chipset. Luminus Devices Inc

Holes for the 12 Volt supply, fan, switches, pin connectors, resistors, and circuit board were drilled with the mill or hand drill in the machine shop. All the wiring cables to the pin connectors are soldered for solid connections. The copper circuit board was milled to alleviate concerns with inconsistent wire contact with components.

3.4 Testing

The experimental testing done so far was a simple examination of the cross flow of ambient air swirled from the air conditioning in the lab. The resistors used were used 3.9 Ω and 2.3 Ω so the LED was running at 4.6 A. This experiment started with the goal of iteratively finding the minimum current the LED would run at to provide sufficient brightness for imaging. The final current value was 24 A which was a considerable jump from 4.6 A.

Chapter 4

Testing Results

4.1 Image Quality

The experimental testing of the second prototype already showed improvements in schlieren imaging, but due to the density variations in the glass panels of the wind tunnels, it was realized that more current would be required to provide even sharper images. Figures 14 and 15 show the images obtained from an experiment run in Mach 1.8 flow with the final prototype. The shocks can be seen quite clearly as vertical lines (note the horizontal lines are due to imperfections in the polycarbonate windows of the wind tunnel).

4.2 Circuit Temperature

At 20 kHz frequency, the circuit can run for approximately 10 minutes before resistors R1 and R2 begin to get warm. However, the greater the TTL pulse frequency the faster the components heat up. This lowers the running time of the circuit and requires longer cooling periods between each experimental run.

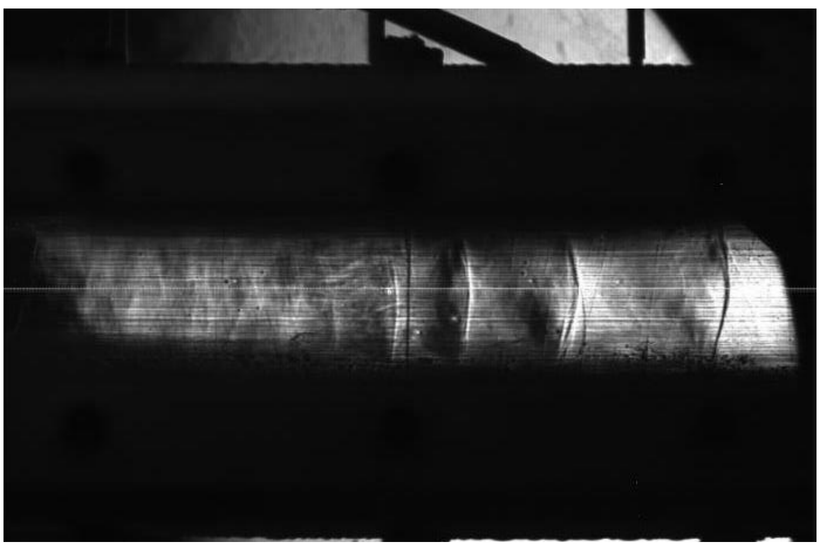

Figure 14

Figure 15

Chapter 5

Conclusions and Future Work

The images pictured above are a good starting point to demonstrate the usability and benefits of the high power pulsed LEDs. The circuit and overall project took many stages of development before a viable product was created. This is less than ideal for the time spent to create one working prototype however, now that various components such as, switches, connectors, and boards are properly specified, a second working prototype can be built in much less time. The integration of the 'Enable Switch' in the final prototype also eliminates the possibility of running the LED continuously which removes the risk of burning out both the LED and the circuit. This also allows the resistance values for R1 and R2 to be further lowered to increase the current to the LED which will output a higher intensity of light. Finally, the more experiments this LED light source is tested on, the more improvements that can be made upon it for high quality schlieren images.

Appendix

Appendix A. LED Specification Sheet

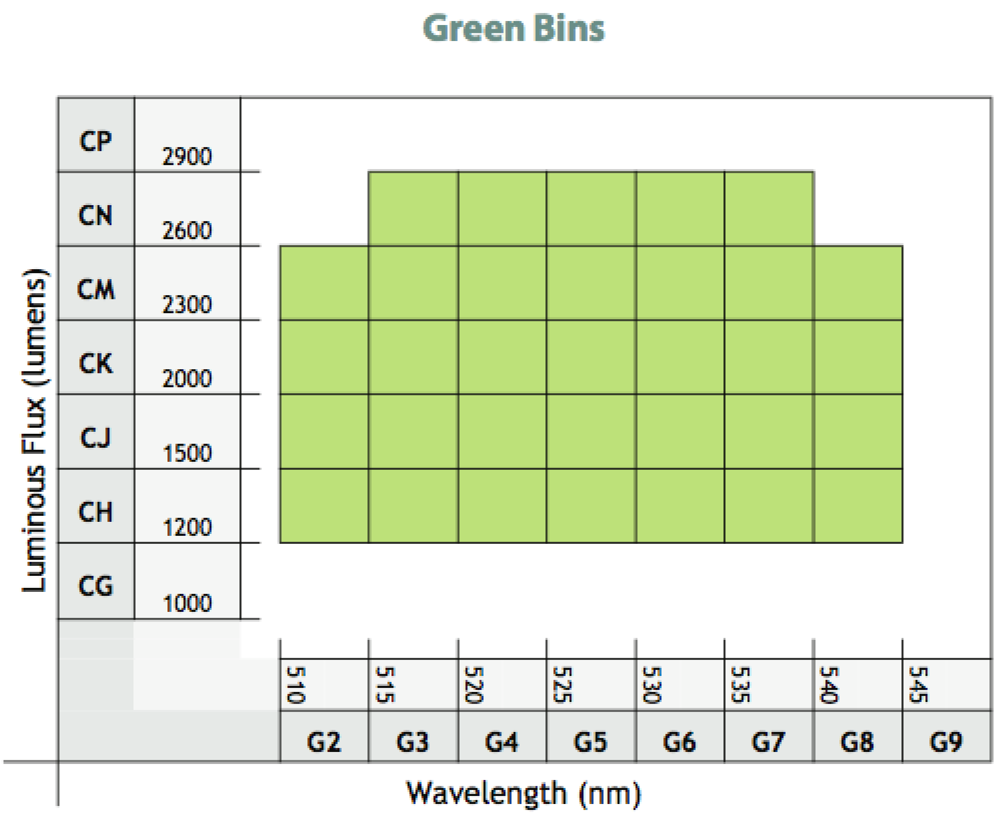

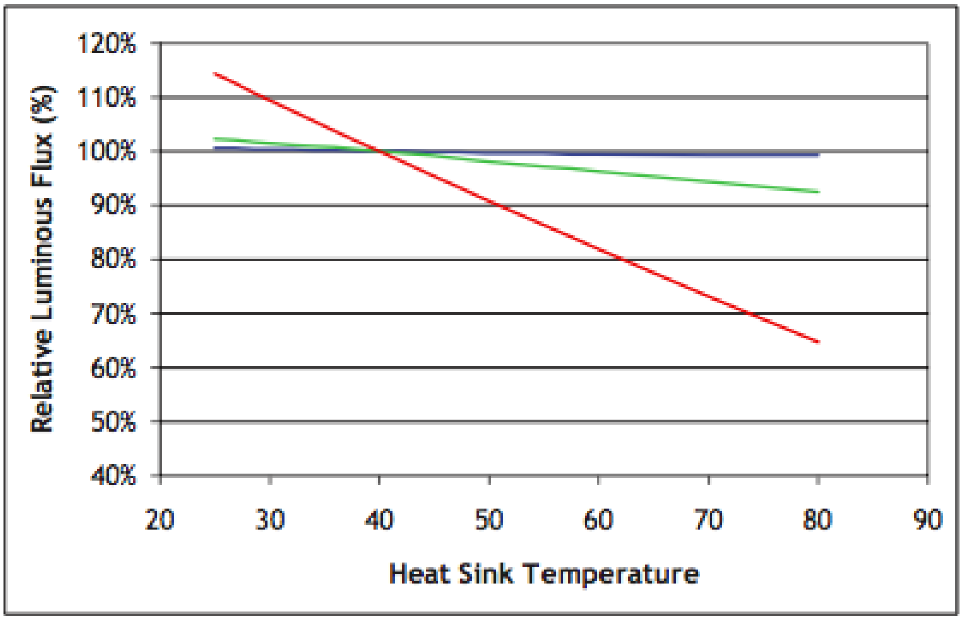

120%
110%
100%
90%
80%
70%
60%
50%
40%
20
30
40
50
60
70
80
90
Relative Luminous Flux (%)
Heat Sink Temperature

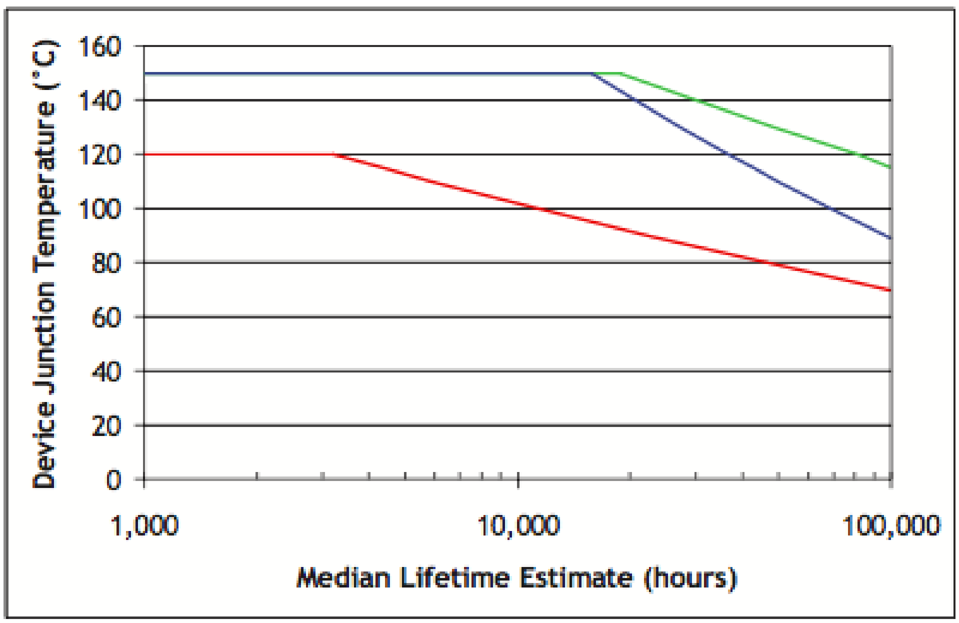

160
140
120
100
80
60
40
20
0
1,000
10,000
100,000
Device Junction Temperature (°C)
Median Lifetime Estimate (hours)

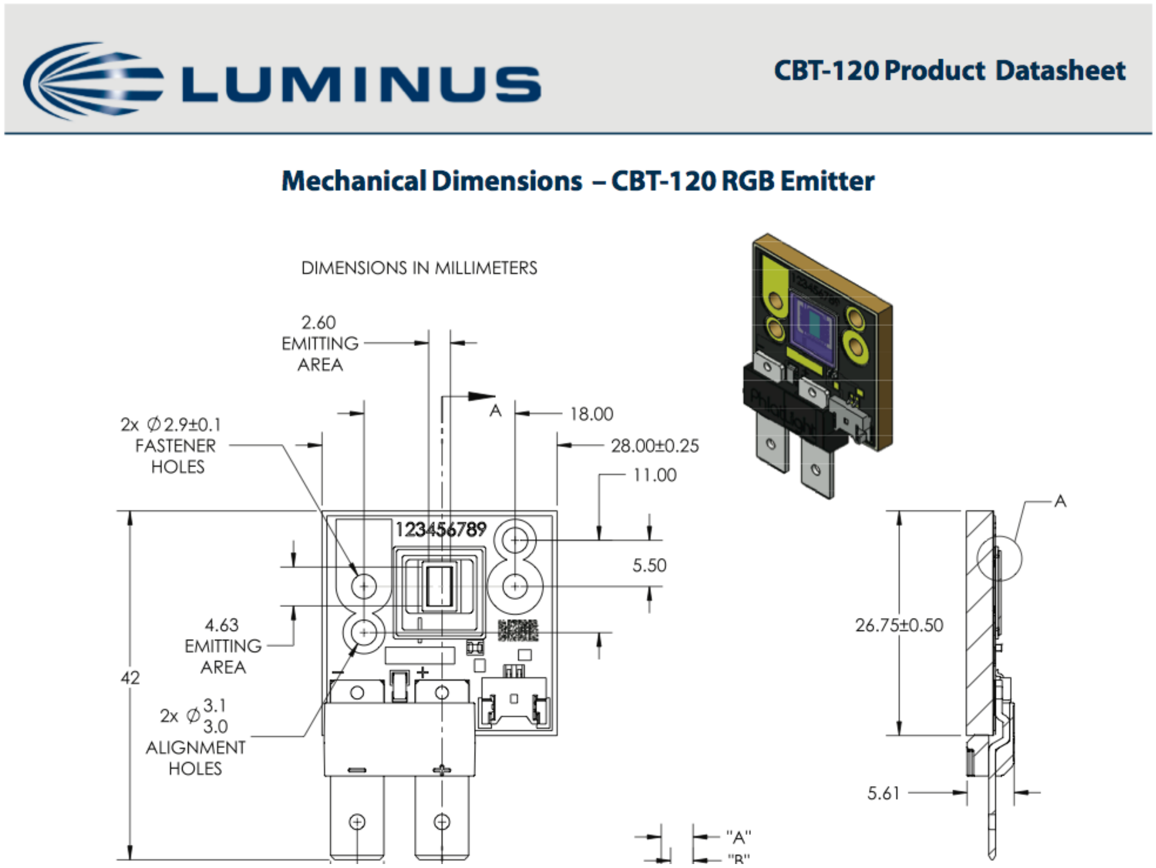

Work Cited

[1] AMES, FORREST E. INTRODUCTION TO COMPRESSIBLE FLOW. BUSINESS EXPERT PRESS, 2017.

[2] Ben-Yakar, A., and R. Hanson. "Ultra-Fast-Framing Schlieren System for Studies of the Time Evolution of Jets in Supersonic Crossflows." *Experiments in Fluids*, vol. 32, no. 6, 20 Apr. 2002, pp. 652–666., doi:10.1007/s00348-002-0405-z.

[3] Bogdonoff, Seymour M. "Some Observations of Three-Dimensional Shock-Wave/Turbulent Boundary-Layer Interactions." Turbulent Shear-Layer/Shock-Wave Interactions, 9 July 2009, pp. 261–272., doi:10.1007/978-3-642-82770-9_21.

[4] Buchmann, Nicolas A., et al. "Pulsed, High-Power LED Illumination for Tomographic Particle Image Velocimetry." *Experiments in Fluids*, vol. 53, no. 5, Oct. 2012, pp. 1545–1560., doi:10.1007/s00348-012-1374-5.

[5] *Exploring in Aeronautics: An Introduction to Aeronautical Sciences*. Rep. no. 89. N.p.: n.p., 1971. *NASA Technical Reports Server*. Web. 6 May 2018.

[6] G. S. Settles. Schlieren and Shadowgraph Techniques. Springer Berlin Heidelberg, first edition, 2001.

[7] Gaitonde, Datta V. "Progress in Shock Wave/Boundary Layer Interactions." *43rd Fluid Dynamics Conference*, 22 Jan. 2013, doi:10.2514/6.2013-2607.

[8] "Laminar and Turbulent Boundary Layers." Classification of Flows, Laminar and Turbulent Flows, 2005, www-mdp.eng.cam.ac.uk/web/library/enginfo/aerothermal_dvd_only/aero/fprops/introvisc/node8.html.

[9] Willert, C, et al. "Pulsed Operation of High-Power Light Emitting Diodes for Imaging Flow Velocimetry." Measurement Science and Technology, vol. 21, no. 7, Aug. 2010, p. 075402., doi:10.1088/0957-0233/21/7/075402.

[10] Willert, Christian E., et al. "An Assessment of High-Power Light-Emitting Diodes for High Frame Rate Schlieren Imaging." Experiments in Fluids, vol. 53, no. 2, May 2012, pp. 413–421., doi:10.1007/s00348-012-1297-1.

[11] "Schlieren System." *NASA*, NASA, 15 May 2015,www.grc.nasa.gov/www/k-12/airplane/tunvschlrn.html.